

## Electronic band structure of highly mismatched GaN<sub>1-x</sub>Sb<sub>x</sub> alloys in a broad composition range

N. Segercrantz, K. M. Yu, M. Ting, W. L. Sarney, S. P. Svensson, S. V. Novikov, C. T. Foxon, and W. Walukiewicz

Citation: *Applied Physics Letters* **107**, 142104 (2015); doi: 10.1063/1.4932592

View online: <http://dx.doi.org/10.1063/1.4932592>

View Table of Contents: <http://scitation.aip.org/content/aip/journal/apl/107/14?ver=pdfcov>

Published by the AIP Publishing

---

### Articles you may be interested in

[Physical properties of Al<sub>x</sub>In<sub>1-x</sub>N thin film alloys sputtered at low temperature](#)

*J. Appl. Phys.* **116**, 153509 (2014); 10.1063/1.4898565

[Ab initio study of the bandgap engineering of Al<sub>1-x</sub>Ga<sub>x</sub>N for optoelectronic applications](#)

*J. Appl. Phys.* **109**, 023109 (2011); 10.1063/1.3531996

[Impact of N- and Ga-face polarity on the incorporation of deep levels in n-type GaN grown by molecular beam epitaxy](#)

*Appl. Phys. Lett.* **96**, 242112 (2010); 10.1063/1.3453660

[Investigation of E<sub>1</sub>\(LO\) phonon-plasmon coupled modes and critical points in In<sub>1-x</sub>Ga<sub>x</sub>N thin films by optical reflectance measurements](#)

*Appl. Phys. Lett.* **96**, 181904 (2010); 10.1063/1.3428368

[Structural and antireflective characteristics of catalyst-free GaN nanostructures on GaN/sapphire template for solar cell applications](#)

*Appl. Phys. Lett.* **96**, 151909 (2010); 10.1063/1.3386538

---

The advertisement features a photograph of the Model PS-100 cryogenic probe station, which is a complex piece of scientific equipment with various mechanical components and a probe. The background is a gradient of blue. The text is arranged around the image: the model name and product description on the left, the company logo and name in the center-right, and a slogan at the bottom right.

**Model PS-100**  
Tabletop Cryogenic  
Probe Station

 **Lake Shore**  
CRYOTRONICS

*An affordable solution for  
a wide range of research*

## Electronic band structure of highly mismatched GaN<sub>1-x</sub>Sb<sub>x</sub> alloys in a broad composition range

N. Segercrantz,<sup>1,2,a)</sup> K. M. Yu,<sup>2,3</sup> M. Ting,<sup>2,4</sup> W. L. Sarney,<sup>5</sup> S. P. Svensson,<sup>5</sup> S. V. Novikov,<sup>6</sup> C. T. Foxon,<sup>6</sup> and W. Walukiewicz<sup>2</sup>

<sup>1</sup>Department of Applied Physics, Aalto University, P.O. Box 14100, FIN-00076 Aalto Espoo, Finland

<sup>2</sup>Materials Sciences Division, Lawrence Berkeley National Laboratory, Berkeley, California 94720, USA

<sup>3</sup>Department of Physics and Materials Science, City University of Hong Kong, Kowloon, Hong Kong

<sup>4</sup>Mechanical Engineering Department, University of California, Berkeley, California 94720, USA

<sup>5</sup>U.S. Army Research Laboratory, 2800 Powder Mill Road, Adelphi, Maryland 20783, USA

<sup>6</sup>School of Physics and Astronomy, University of Nottingham, Nottingham NG7 2RD, United Kingdom

(Received 15 July 2015; accepted 25 September 2015; published online 6 October 2015)

In this letter, we study the optical properties of GaN<sub>1-x</sub>Sb<sub>x</sub> thin films. Films with an Sb fraction up to 42% were synthesized by alternating GaN-GaSb layers at a constant temperature of 325 °C. The measured optical absorption data of the films are interpreted using a modified band anticrossing model that is applicable to highly mismatched alloys such as GaN<sub>1-x</sub>Sb<sub>x</sub> in the entire composition range. The presented model allows us to more accurately determine the band gap as well as the band edges over the entire composition range thereby providing means for determining the composition for, e.g., efficient spontaneous photoelectrochemical cell applications. © 2015 AIP Publishing LLC. [<http://dx.doi.org/10.1063/1.4932592>]

Recent progress in non-equilibrium epitaxial growth techniques enabled synthesis of semiconductor materials with unique electrical and optical properties. Thus, with a proper control of the growth temperature and fluxes it has become possible to synthesize highly mismatched alloys (HMAs) in the whole composition range.<sup>1,2</sup> This has greatly expanded the range of possible semiconductor materials whose electronic band structure can be tailored for specific applications.<sup>3,4</sup> It has been shown that dilute group III-V nitrides<sup>5,6</sup> and dilute group II-VI oxides<sup>7</sup> have the energy band structure suitable for intermediate band solar cells. The large redshift measured for dilute GaN<sub>x</sub>Sb<sub>1-x</sub> and GaN<sub>x</sub>As<sub>1-x</sub>, in turn, makes these alloys interesting for mid- and long-wavelength infrared applications.<sup>8-13</sup>

Recently, GaN-based HMAs have been proposed as good candidates for photoelectrochemical (PEC) cells for solar water dissociation. There are two key requirements in terms of the electronic band structure for the semiconductor materials to be suitable for solar water splitting applications. First, the band gap has to be small enough to absorb a significant portion of the solar spectrum, and second, the band edges have to straddle the redox potentials with the conduction band edge (CBE) located above the hydrogen reduction and the valence band edge (VBE) below the water oxidation potential.<sup>14</sup> These conditions are difficult to satisfy and a significant effort was extended into finding suitable semiconductors. Besides a high mechanical hardness and a chemical stability, the fact that the band gap and the band offsets of GaN-based alloys can be tuned by replacing the N anion with other group V elements, e.g., with As, Bi, and Sb<sup>12,15-17</sup> makes these alloyed interesting for PEC applications. Such HMAs are however difficult to synthesize because of the limited solubility under equilibrium conditions. The miscibility gap has recently been overcome using low temperature

molecular beam epitaxy (LT-MBE) growth, allowing synthesis of GaN<sub>1-x</sub>As<sub>x</sub> over the whole composition range<sup>1,18</sup> and of GaN<sub>1-x</sub>Sb<sub>x</sub> with Sb fractions up to 66%.<sup>2,19</sup> Although amorphous in the composition range 0.10 < x < 0.8, the GaN<sub>1-x</sub>As<sub>x</sub> films exhibited well-defined absorption edges in the energy range of 3.4 eV for GaN to ~0.85 eV for x = 0.8.

Even larger band gap reductions were measured for the GaN<sub>1-x</sub>Sb<sub>x</sub> films. In films grown under Ga-rich conditions, the optical properties were dominated by defect states and the absorption edge was not very sensitive to the Sb concentration.<sup>20</sup> However, for films grown under N-rich conditions, the sole factor determining the width of the band gap was shown to be the Sb concentration.<sup>15,21</sup> The Sb incorporation could be enhanced by using extremely low growth temperatures (~80 °C) and by increasing the Sb BEP (beam equivalent pressure). Similar to the GaN<sub>1-x</sub>As<sub>x</sub> films, sharp optical absorption edges shifting towards energies of ~0.6 eV at x = 0.66 were measured for the GaN<sub>1-x</sub>Sb<sub>x</sub> films exhibiting an amorphous structure for x > 0.06. The measured results indicate a short-range order for the amorphous films resembling random crystalline HMAs.

All the potential applications of the HMAs require a good understanding of the electronic band structure and knowledge of the location of the band edges on the absolute scale, i.e., relative to the vacuum level. Previously, the composition dependencies of the valence and conduction band edges were calculated by compositional weighting of the band anticrossing (BAC) model derived for dilute alloys at the end compounds. This approximation is not suitable for the HMAs with localized levels located in the band gap of the host semiconductor matrix and, as has been shown in Ref. 2, it significantly overestimates the band gap reduction in the mid composition range. To date, the BAC model is however the only model striving to explain the band gap variation over the whole composition range for the HMAs such as GaNSb. Although some first principle calculations

<sup>a)</sup>natalie.segercrantz@aalto.fi

exist on dilute  $\text{GaN}_{1-x}\text{Sb}_x$ ,<sup>22,23</sup> the calculated band gaps are clearly smaller than the experimentally observed ones.<sup>2</sup>

In this letter, we present a comprehensive study of the optical properties of  $\text{GaN}_{1-x}\text{Sb}_x$  HMAs grown by intermixing of GaN–GaSb multilayer structures. The measured optical absorption results are interpreted using a modified BAC model that is applicable to the HMAs in the entire composition range. The band gap as well as the band offsets of the HMAs can be more precisely determined using this model. The study allows determination of the alloy composition range suitable for PEC applications.

The  $\text{GaN}_{1-x}\text{Sb}_x$  films were synthesized by growing a multilayer structure with a number of alternating layers of GaN and GaSb using MBE on a sapphire substrate at a constant temperature of 325 °C. The average composition was controlled by the GaN to GaSb layer thickness ratio. An intermixing of the layers produced alloys with thicknesses of 150–300 nm and Sb compositions up to  $x = 0.42$ . The composition and the thickness of the films were determined using Rutherford Backscattering Spectrometry (RBS). The RBS data show compositional uniformity along the growth direction for all samples. Transmission electron microscopy (TEM) images show crystalline films and no phase separation for samples with less than 18% Sb. A weak periodic structure consisting of very small polycrystalline-amorphous grains could be seen in the TEM images of the sample with 18% Sb. The only sample showing Sb segregation is the thin film with 42% Sb. This sample is a mix of polycrystalline and amorphous GaNSb. However, this thin film shows no evidence of a periodic structure. The films were found to be highly resistive with the exception of samples with higher Sb content that show weak  $p$ -type conductivity. More details of the crystal growth and structural characterization will be presented elsewhere.<sup>24</sup>

The optical properties of the films were studied by optical transmission and reflection in the spectral range of 250–2500 nm using a Perkin Elmer Lambda 950 Spectrophotometer. Figure 1 illustrates the measured absorption spectra for five of the eight  $\text{GaN}_{1-x}\text{Sb}_x$  thin films with compositions ranging from  $x = 0$  to 0.42. As can be seen from the figure, the absorption spectra of the pure GaN film

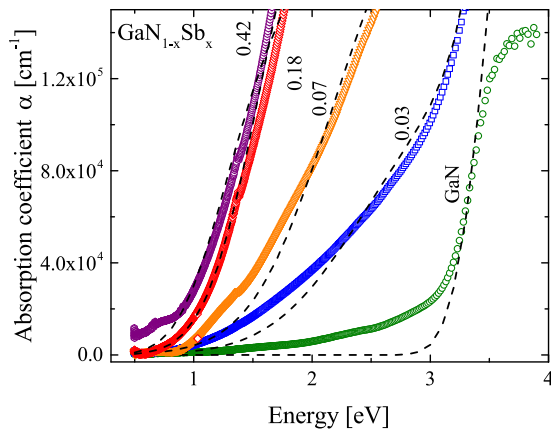


FIG. 1. The measured (circles) and fitted (black dashed lines) absorption coefficients using our modified BAC model for five of the  $\text{GaN}_{1-x}\text{Sb}_x$  thin films.

lack a sharp onset. Instead, a weak absorption tail beginning at roughly 1 eV is seen for this sample. Since the thin films are grown under slightly Ga-rich conditions, we associate the absorption tail with similar type of defects as seen in the absorption spectra for the  $\text{GaN}_{1-x}\text{Sb}_x$  films grown by LT-MBE under Ga-rich conditions in Ref. 20. However, in contrast to the earlier studied Ga-rich samples, as the Sb fraction is increased the absorption coefficient increases and the sub-band gap absorption edge shifts to lower energies and becomes more dominant at higher Sb contents. This type of behavior was also seen for the LT-MBE  $\text{GaN}_{1-x}\text{Sb}_x$  thin films grown under N-rich conditions in Ref. 2. Despite the very different growth methods, the measured absorption spectra of the N-rich LT-MBE grown films agree very well with those of the thin films studied in this work. This gives evidence that the growth method of multilayer intermixing presented in this letter can be used for reliably growing  $\text{GaN}_{1-x}\text{Sb}_x$  thin films with high Sb contents.

In order to explain the measured results, we have to account for the variation of the band gap in the whole composition range. The BAC model describes well the composition dependence of the band energies in the dilute composition limits, i.e., a small N content in GaSb (conduction band anti-crossing) and a small Sb content in GaN (valence band anti-crossing). The band edge energies for these dilute ternary compounds are given by<sup>25–27</sup>

$$E_V^+(k) = \frac{1}{2} \left[ (E_{\text{Sb}} + E_V(k)) + \sqrt{(E_V(k) - E_{\text{Sb}})^2 + 4C_{\text{Sb}}^2 x} \right], \quad (1)$$

$$E_C^-(k) = \frac{1}{2} \left[ (E_{\text{N}} + E_C(k)) - \sqrt{(E_C(k) + E_{\text{N}})^2 + 4C_{\text{N}}^2 (1-x)} \right], \quad (2)$$

where  $x$  denotes the Sb concentration, and  $E_{\text{Sb}}$  and  $E_{\text{N}}$  are the energy levels of Sb and N, respectively. In the dilute composition limit, it was possible to assume that the valence and conduction matrix band edges  $E_V(k)$  and  $E_C(k)$  and their respective coupling parameters  $C_{\text{Sb}}$  and  $C_{\text{N}}$  are not composition dependent.

The simplest way to extend the BAC model was to compositionally weight the BAC results obtained in the dilute limits to the whole composition range.<sup>28</sup> The approach predicted overall trends but significantly overestimated the band gap reductions for alloys with mid-range compositions. The main deficiencies of the model were that it ignored the composition dependence of the coupling parameter and assumed that the BAC interactions fully determine the shifts of the conduction and the valence band edge. To correct the deficiencies, we adopt here a hybrid model assuming that the band structure of the host crystal is given by the virtual crystal approximation. This allows the BAC interactions to be treated as perturbations. In this approach, the valence and conduction matrix band edges are given by the linear interpolation between the end point compounds

$$E_V(x, k = 0) = (1-x)E_{V, \text{GaN}} - xE_{V, \text{GaSb}}, \quad (3)$$

$$E_C(x, k = 0) = (1-x)E_{C, \text{GaN}} - xE_{C, \text{GaSb}}, \quad (4)$$

where  $E_{V,\text{GaN}}$  and  $E_{V,\text{GaSb}}$  denote the VBEs, and  $E_{C,\text{GaN}}$  and  $E_{C,\text{GaSb}}$  of the CBEs of GaN and GaSb, respectively. Also in the virtual crystal approximation, the potential of the anion lattice site for the  $\text{GaN}_{1-x}\text{Sb}_x$  alloy is given by the average potential

$$V_{\text{vc}}(x) = (1-x)V_{\text{N}} + xV_{\text{Sb}}, \quad (5)$$

where  $V_{\text{N}}$  and  $V_{\text{Sb}}$  are the N and the Sb potentials, respectively. In this approximation, the composition dependencies of the coupling parameters for  $\text{GaN}_{1-x}\text{Sb}_x$  are given by  $C_{\text{N}}(x) = xC_{\text{N}_0}$  and  $C_{\text{Sb}}(x) = (1-x)C_{\text{Sb}_0}$ .  $C_{\text{Sb}_0}$  and  $C_{\text{N}_0}$  are, respectively, the coupling constants in the dilute N and Sb composition limits.

Figure 2(a) illustrates the band structure of a  $\text{GaN}_{0.72}\text{Sb}_{0.18}$  alloy calculated using our modified BAC model. For all calculations presented in this letter,  $E_{\text{Sb}}$  was at 1.2 eV above the VBE of GaN and  $E_{\text{N}}$  at 0.45 eV above the CBE of GaSb. The values  $C_{\text{N}_0} = 2.7$  eV and  $C_{\text{Sb}_0} = 2.5$  eV were used for the constants describing the BAC couplings.<sup>2</sup> The latter coupling constant was obtained from fitting the measured absorption coefficients in this letter. As seen in the figure, since the  $p$ -like states of elemental Sb have a relatively large spin-orbit splitting energy of 0.75 eV<sup>29,30</sup> the optical transitions from this band is considered as well. The band gap energy for the alloys is defined as the energy difference between the  $E_{+}^{\text{V}}(k)$  and the  $E_{-}^{\text{C}}(k)$  band.

The optical absorption coefficient is proportional to the joint optical density of states and the dipole matrix element between initial and final states. To evaluate the absorption coefficient in the  $\text{GaN}_{1-x}\text{Sb}_x$  alloys using our modified BAC model, six optical transitions from three valences to two conduction sub-bands were considered. For example, as shown in Fig. 2(b), the optical absorption coefficient associated with transitions from the higher valence band  $E_{+}^{\text{V}}(k)$  to the lower conduction band  $E_{-}^{\text{C}}(k)$  is proportional to the corresponding joint density of states and can be written as

$$g_{+}^{-}(\hbar\omega) = \frac{1}{4\pi\sqrt{\pi}(\Delta_{\text{C}}^{-} + \Delta_{\text{V}}^{+})} \int \sin\left(\frac{\theta_{\text{V}}}{2}\right)^2 \sin\left(\frac{\theta_{\text{C}}}{2}\right)^2 \times \exp\left(-\left(\frac{\hbar\omega - [E_{-}^{\text{C}}(k) - E_{+}^{\text{V}}(k)]}{\Delta_{\text{C}}^{-} + \Delta_{\text{V}}^{+}}\right)^2 k^2 dk\right), \quad (6)$$

where  $\Delta_{\text{C}}^{-}$  and  $\Delta_{\text{V}}^{+}$  are the broadening parameters of  $E_{+}^{\text{V}}(k)$  and  $E_{-}^{\text{C}}(k)$ , respectively. The broadening effects caused by the alloy inhomogeneity are incorporated by convoluting the density of states with a Gaussian function at each value of  $k$ . In addition, we have assumed that there is no optical coupling between extended and localized states, therefore the optical absorption is proportional to the delocalized part of the wavefunction of a given sub-band. This effect is accounted for by the first two factors under the integral in Eq. (6).<sup>26</sup>

The expression for the total absorption coefficient includes the six transitions described above, with each transition  $i$  weighted by its degeneracy factor  $g_i$  as  $\sum_{i=1}^6 \alpha_0 g_i g_i(\hbar\omega)$ .  $\alpha_0$  is a scaling constant obtained by fitting the experimental absorption spectrum. In Fig. 2(b), the calculated total absorption coefficient for the  $\text{GaN}_{0.82}\text{Sb}_{0.18}$  thin film along with the six different contributions is illustrated.

The total calculated absorption coefficients for five of the  $\text{GaN}_{1-x}\text{Sb}_x$  films using the modified BAC model are shown as the dashed lines in Fig. 1 together with the experimental data. From the calculated absorption coefficients fitted to the measured ones, we determine the coupling constant of Sb to be  $C_{\text{Sb}_0} = 2.5$  eV. The broadening parameters vary 0.01 – 0.5 eV. The sample with the highest Sb fraction,  $x = 0.42$ , could not be fitted using the same coupling constant. The explanation for this is the segregation of Sb seen in the TEM measurements of this sample. The substitutional Sb concentration in this sample is therefore expected to be lower than the 42% measured by the RBS.

In Fig. 3, the band gaps obtained from fitting the absorption coefficients for the  $\text{GaN}_{1-x}\text{Sb}_x$  thin films using our modified BAC model are shown along with the band gaps from previous studies of  $\text{GaN}_{1-x}\text{Sb}_x$ <sup>2</sup> and of dilute-N GaSb.<sup>9</sup> With the known BAC parameters, we can calculate the band gap energy as well as energies of the conduction and the valence band edges on the absolute scale in the whole  $\text{GaN}_{1-x}\text{Sb}_x$  alloy composition range. This is also illustrated in Fig. 3 along with the band gap predicted by the original BAC model in Ref. 2. The inset in Fig. 3 illustrates the positions of the CBE and the VBE predicted by the two models. As can be seen in the figure, the modified model provides a much better fit to the experimentally determined gaps and predicts a smaller downward shift of the CBE as a function of Sb content.

Spontaneous water splitting requires that the band edges of a semiconductor material straddle the water redox potentials.<sup>14</sup> As is seen in Fig. 3, the modified BAC model predicts that in the case of  $\text{GaN}_{1-x}\text{Sb}_x$  alloys this condition is satisfied for  $x$  up to 0.2 and with the gap as low as 1.3 eV. In contrast, the old BAC model predicted the band edges to straddle the redox potential only for  $x < 0.12$ . Therefore, the modified model considerably extends the composition range of the alloys suitable for efficient spontaneous PEC applications.

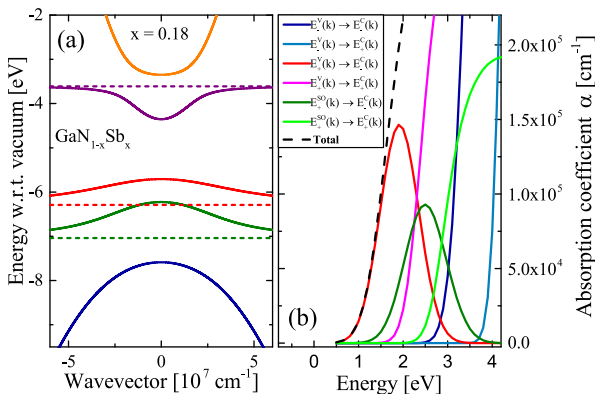


FIG. 2. (a) The band structure of a  $\text{GaN}_{0.82}\text{Sb}_{0.18}$  alloy calculated using our modified BAC model. The dotted lines indicate the localized levels of the N and the Sb atoms as well as the Sb spin-orbit level. The dashed black lines show the dispersions of the valence, conduction, and the spin-orbit split-off bands of the host matrix. (b) The black dashed line represents the calculated absorption coefficient  $\alpha$  for the  $\text{GaN}_{0.72}\text{Sb}_{0.18}$  film using our modified BAC model. The contributions of the six different optical transitions are also shown.

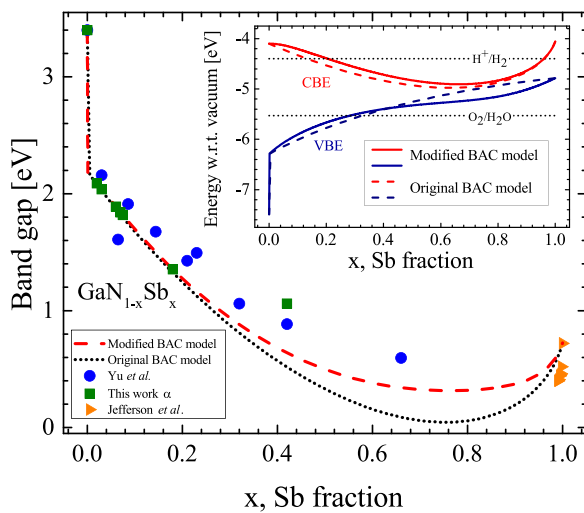


FIG. 3. Fitted band gap energies for the  $\text{GaN}_{1-x}\text{Sb}_x$  films compared to earlier studied  $\text{GaN}_{1-x}\text{Sb}_x$  thin films by Yu *et al.*<sup>2</sup> Band gap energies for GaSb-rich alloys with up to 1% of N were taken from Ref. 9. The band gap energy over the whole composition range was calculated using our modified BAC model (dashed red line) and compared to the band gap calculated using the original model in Ref. 2 (dotted black line). The inset shows the VBE and CBE over the whole composition range using both our modified BAC model (solid lines) and the original BAC model (dashed line). The Redox levels for  $\text{pH} = 2$  are indicated as dotted lines in the inset.

The significance of the modified BAC model presented in this letter is that it not only provides a good fit for the optical gap, but also more accurately predicts the structures of the conduction and valence band. This greatly expands the range of compositions of these alloys that could be used for spontaneous solar water splitting. An important feature of the modified BAC model is thus that it predicts smaller band gap reductions and could provide a better explanation for the composition dependence previously observed in other HMAs including GaNAs, ZnOTe, and ZnOSe.<sup>1,31–33</sup>

In summary, we have studied the optical properties of GaNSb alloys grown by a multilayer method. The composition dependence of the optical absorption edge of the alloy is explained by a modified BAC model that allows for a more accurate determination of the band gap energy and the locations of the band edges relative to the water redox potentials. From our study, we conclude that the GaNSb alloy is a promising candidate for PEC applications with Sb compositions up to 20%.

RBS, optical measurements and the data analysis performed at LBNL were supported by the Director, Office of Science, Office of Basic Energy Sciences, Materials Sciences and Engineering Division, of the U.S. Department of Energy under Contract No. DE-AC02-05CH11231. The sample growth was performed by U.S. Army Research Laboratory.

<sup>1</sup>K. M. Yu, S. V. Novikov, R. Broesler, I. N. Demchenko, J. D. Denlinger, Z. Liliental-Weber, F. Luckert, R. W. Martin, W. Walukiewicz, and C. Foxon, *J. Appl. Phys.* **106**, 103709 (2009).

<sup>2</sup>K. M. Yu, S. V. Novikov, M. Ting, W. L. Sarney, S. P. Svensson, M. Shaw, R. W. Martin, W. Walukiewicz, and C. T. Foxon, *J. Appl. Phys.* **116**, 123704 (2014).

- <sup>3</sup>N. López, L. A. Reichertz, K. M. Yu, K. Campman, and W. Walukiewicz, *Phys. Rev. Lett.* **106**, 028701 (2011).
- <sup>4</sup>K. M. Yu, W. Walukiewicz, J. W. Ager III, D. Bour, R. Farshchi, O. D. Dubon, S. X. Li, I. D. Sharp, and E. E. Haller, *Appl. Phys. Lett.* **88**, 092110 (2006).
- <sup>5</sup>H. P. Nair, A. M. Crook, K. M. Yu, and S. R. Bank, *Appl. Phys. Lett.* **100**, 021103 (2012).
- <sup>6</sup>N. Ahsan, N. Miyashita, M. M. Islam, K. M. Yu, W. Walukiewicz, and Y. Okada, *Appl. Phys. Lett.* **100**, 172111 (2012).
- <sup>7</sup>T. Tanaka, K. M. Yu, A. X. Levander, O. D. Dubon, L. A. Reichertz, N. Lopez, M. Nishio, and W. Walukiewicz, *Jpn. J. Appl. Phys.* **50**, 082304 (2011).
- <sup>8</sup>T. D. Veal, L. F. J. Piper, S. Jollands, B. R. Bennett, P. H. Jefferson, P. A. Thomas, C. F. McConville, B. N. Murrin, L. Buckle, G. W. Smith *et al.*, *Appl. Phys. Lett.* **87**, 132101 (2005).
- <sup>9</sup>P. H. Jefferson, T. D. Veal, L. F. J. Piper, B. R. Bennett, C. F. McConville, B. Murrin, L. Buckle, G. Smith, and T. Ashley, *Appl. Phys. Lett.* **89**, 111921 (2006).
- <sup>10</sup>A. Belabbes, M. Ferhat, and A. Zaoui, *Appl. Phys. Lett.* **88**, 152109 (2006).
- <sup>11</sup>D. Wang, S. P. Svensson, L. Shterengas, G. Belenky, C. S. Kim, I. Vurgaftman, and J. R. Meyer, *J. Appl. Phys.* **105**, 014904 (2009).
- <sup>12</sup>K. Uesugi, N. Morooka, and I. Suemune, *Appl. Phys. Lett.* **74**, 1254 (1999).
- <sup>13</sup>F. Bousbih, S. B. Bouzid, R. Ctourou, F. F. Charfi, J. C. Harmand, and G. Ungaro, *Mater. Sci. Eng., C* **21**, 251 (2002).
- <sup>14</sup>T. Bak, J. Nowotny, M. Rekas, and C. C. Sorrell, *Int. J. Hydrogen Energy* **27**, 991 (2002).
- <sup>15</sup>S. V. Novikov, M. Y. Kin, A. Levander, D. Detert, W. L. Sarney, Z. Liliental-Weber, M. Shaw, R. W. Martin, S. P. Svensson, W. Walukiewicz *et al.*, *J. Vac. Sci. Technol., B* **31**, 03C102 (2013).
- <sup>16</sup>A. X. Levander, K. M. Yu, S. V. Novikov, A. Tseng, C. T. Foxon, O. D. Dubon, J. Wu, and W. Walukiewicz, *Appl. Phys. Lett.* **97**, 141919 (2010).
- <sup>17</sup>S. V. Novikov, C. R. Staddon, C. T. Foxon, K. M. Yu, R. Broesler, M. Hawkrige, Z. Liliental-Weber, J. Denlinger, I. Demchenko, F. Luckert *et al.*, *J. Cryst. Growth* **323**, 60 (2011).
- <sup>18</sup>K. M. Yu, S. V. Novikov, R. Broesler, Z. Liliental-Weber, A. X. Levander, V. M. Kao, O. D. Dubon, J. Wu, W. Walukiewicz, and C. T. Foxon, *Appl. Phys. Lett.* **97**, 101906 (2010).
- <sup>19</sup>K. M. Yu, W. L. Sarney, S. V. Novikov, D. Detert, R. Zhao, J. D. Denlinger, S. P. Svensson, O. D. Dubon, W. Walukiewicz, and C. T. Foxon, *Appl. Phys. Lett.* **102**, 102104 (2013).
- <sup>20</sup>W. L. Sarney, S. P. Svensson, S. V. Novikov, K. M. Yu, W. Walukiewicz, and C. T. Foxon, *J. Cryst. Growth* **383**, 95 (2013).
- <sup>21</sup>W. L. Sarney, S. P. Svensson, S. V. Novikov, K. M. Yu, W. Walukiewicz, M. Ting, and C. T. Foxon, *J. Cryst. Growth* **425**, 255 (2015).
- <sup>22</sup>R. M. Sheetz, E. Richter, A. N. Andriotis, S. Lisenkov, C. Pendyala, M. K. Sunkara, and M. Menon, *Phys. Rev. B* **84**, 075304 (2011).
- <sup>23</sup>A. N. Andriotis, R. M. Sheetz, E. Richter, and M. Menon, *J. Phys.: Condens. Matter* **26**, 055013 (2014).
- <sup>24</sup>W. L. Sarney, S. P. Svensson, N. Segercrantz, M. Ting, W. Walukiewicz, K. M. Yu, R. W. Martin, S. V. Novikov, and C. T. Foxon, "Intermixing studies in  $\text{GaN}_{1-x}\text{Sb}_x$  highly mismatched alloys," *Phys. Status Solidi B* (submitted).
- <sup>25</sup>K. Alberi, J. Wu, W. Walukiewicz, K. M. Yu, O. D. Dubon, S. P. Watkins, C. X. Wang, X. Liu, Y.-J. Cho, and J. Furdyna, *Phys. Rev. B* **75**, 045203 (2007).
- <sup>26</sup>M. A. Mayer, P. R. Stone, N. Miller, H. M. Smith III, O. D. Dubon, E. E. Haller, K. M. Yu, W. Walukiewicz, X. Liu, and J. K. Furdyna, *Phys. Rev. B* **81**, 045205 (2010).
- <sup>27</sup>J. Wu, W. Shan, and W. Walukiewicz, *Semicond. Sci. Technol.* **17**, 860 (2002).
- <sup>28</sup>C.-Z. Zhao, N.-N. Li, T. Wei, S.-S. Wang, and K.-Q. Lu, *Appl. Phys. A* **115**, 927 (2014).
- <sup>29</sup>J. E. Peralta, J. Heyd, G. E. Scuseria, and R. L. Martin, *Phys. Rev. B* **74**, 073101 (2006).
- <sup>30</sup>M. Cardona, N. E. Christensen, and G. Fasol, *Phys. Rev. B* **38**, 1806 (1988).
- <sup>31</sup>M. Ting, R. dos Reis, M. Jaquez, O. D. Dubon, S. S. Mao, K. M. Yu, and W. Walukiewicz, *Appl. Phys. Lett.* **106**, 092101 (2015).
- <sup>32</sup>W. Shan, W. Walukiewicz, J. Ager III, K. M. Yu, J. Wu, E. E. Haller, Y. Nabetani, T. Mukawa, Y. Ito, and T. Matsumoto, *Appl. Phys. Lett.* **83**, 299 (2003).
- <sup>33</sup>M. A. Mayer, D. T. Speaks, K. M. Yu, S. S. Mao, E. E. Haller, and W. Walukiewicz, *Appl. Phys. Lett.* **97**, 022104 (2010).